ACS chemical biology

Letters

pubs.acs.org/acschemicalbiology

Rational Design of Small-Molecule Inhibitors for β-Catenin/T-Cell Factor Protein−Protein Interactions by Bioisostere Replacement

Binxun Yu, Zheng Huang, Min Zhang, Darren R. Dillard, and Haitao Ji*

Department of Chemistry, Center for Cell and Genome Science, University of Utah, Salt Lake City, Utah 84112-0850, United States

Supporting Information

ABSTRACT: A new hot spot-based design strategy using bioisostere replacement is reported to rationally design nonpeptidic small-molecule inhibitors for protein−protein interactions. This method is applied to design new potent inhibitors for β-catenin/T-cell factor (Tcf) interactions. Three hot spot regions of Tcf for binding to β-catenin were quantitatively evaluated; the key binding elements around K435 and K508 of β-catenin were derived; a bioisostere library was used to generate new fragments that can match the proposed critical binding elements. The most potent inhibitor, with a molecular weight of 230, has a K_d of 0.531 μM for binding to β-catenin and a K_i of 3.14 μM to completely disrupt β-catenin/Tcf interactions. The binding mode of the designed inhibitors was validated by the site-directed mutagenesis and structure−activity relationship (SAR) studies. This study provides a new approach to design new small-molecule inhibitors that bind to β-catenin and effectively disrupt β-catenin/Tcf interactions specific for canonical Wnt signaling.

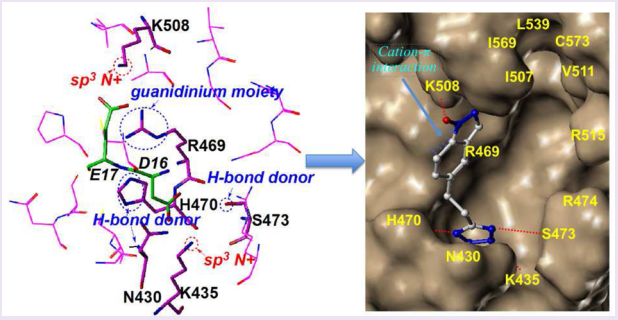

Protein−protein interactions (PPIs) are of utmost importance for all living organisms.[1] Abnormal PPIs are often the key steps for the pathological processes. However, searching for small-molecule PPI inhibitors has proven to be challenging. Protein hot spots (small subsets of protein surface residues contribute to most of the free energy of binding)[2] can serve as the starting point for the rational design of potent PPI inhibitors, which leads to the generation of three approaches: virtual screening,[3] fragment screening,[4] and hot spot-based design.[5−7] The current hot spot-based design strategy extracts key substructures from the hot spot residues and directly derivatizes them to a more potent PPI inhibitor. For example, the indole or phenyl ring of W23 of p53 was employed to generate the potent inhibitors for p53/MDM2 PPIs;[5,6] the 4-hydroxyl-L-proline of hypoxia-inducible factor 1α (HIF-1α) was used as the key binding moiety to build potent inhibitors for von hippel-Lindau protein (VHL)/HIF-1α interactions.[7] The substructures from the hot spot residues clearly lie in the optimized inhibitors. Herein, we report a new hot spot-based design strategy using the bioisostere replacement technique to generate new potent small-molecule PPI inhibitors with new structures. As a first case study, this approach is applied to the design of novel nonpeptidic and low-molecular-weight inhibitors for β-catenin/T-cell factor (Tcf) PPIs, a key site in the downstream of the canonical Wnt signaling pathway.

The canonical Wnt/β-catenin signaling pathway plays a pivotal role in the regulation of cell growth, differentiation, and cell−cell communication.[8] The aberrant activation of canonical Wnt/β-catenin signaling drives the initiation and progression of many cancers, including colorectal and hepatocellular carcinomas, and pulmonary fibroses. Transcriptional overactivation of Wnt/β-catenin target genes is solely dependent on the formation of the β-catenin/Tcf complex. Selective inhibition of β-catenin/Tcf PPIs represents an appealing therapeutic target. Furthermore, it would be ideal that the inhibitor binds to coactivator β-catenin rather than transcriptional factor Tcf, as Tcf is essential in other signaling pathways, while β-catenin is specific for Wnt/β-catenin signaling. Crystal structures of β-catenin in complexes with *Xenopus* Tcf3,[9] human Tcf4,[10−12] and mouse Lef-1[13] have been reported. These structures reveal a large protein−protein contacting surface between β-catenin and Tcf (≥2800 Å^2 versus typical PPI surfaces of 1500−3000 Å^2). Biochemical analyses indicate that the dissociation constant (K_d) value of β-catenin/Tcf PPIs is in the 7−10 nM range.[13,14] To disrupt such a large and tightly binding complex requires an extraordinarily high ligand efficiency of small molecule. Up to date, no structure-based design of small-molecule inhibitors has been reported. Only four high-throughput screenings (HTSs) were reported.[15−18] However, to which proteins of β-catenin and Tcf as well as the exact location on protein the known inhibitors bind was unknown, which have prohibited the further optimization of those HTS hits. The hydrocarbon-stapled Axin α-helix peptides were recently reported to bind to β-catenin Axin-binding site and inhibit β-catenin/Tcf interactions.[19] Axin is the scaffolding protein for β-catenin phosphorylation. β-catenin/Axin PPIs

Received: October 18, 2012
Accepted: December 28, 2012
Published: December 28, 2012

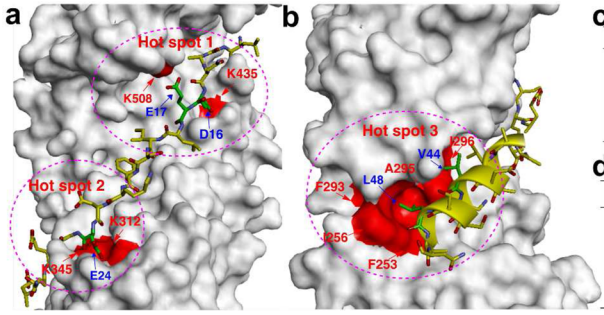

c

No.	Peptides	K_d, nM
1	Tcf4 (residues 7-51)	4.71
2	Tcf4 (residues 7-51, D16A, E17A)	>100,000
3	Tcf4 (residues 7-51, E24A, E29A)	28
4	Tcf4 (residues 7-51, V44A, L48A)	89.3

d

No.	Peptides	IC_{50}, nM
1	Tcf4 (residues 7-51)	1.09 ± 0.042
2	Tcf4 (residues 7-31)	427.7 ± 5.58
3	Tcf4 (residues 7-51, D16A, E17A)	>200,000
4	Tcf4 (residues 7-51, E24A, E29A)	68.07 ± 2.46
5	Tcf4 (residues 7-51, V44A, L48A)	606.1 ± 1.54

Figure 1. (a) Hot spots 1 and 2. β-Catenin is shown as a surface model (gray), and Tcf is shown as a stick model (PDB id, 2GL7[12]). Hot spot 1 includes K435 and K508; hot spot 2 includes K312 and K345. (b) Hot spot 3. It includes F253, I256, F293, A295, and I296. (c) SPR study of β-catenin with wild-type and mutant Tcf4 peptides. (d) FP competitive inhibition assay of unlabeled Tcf peptides.

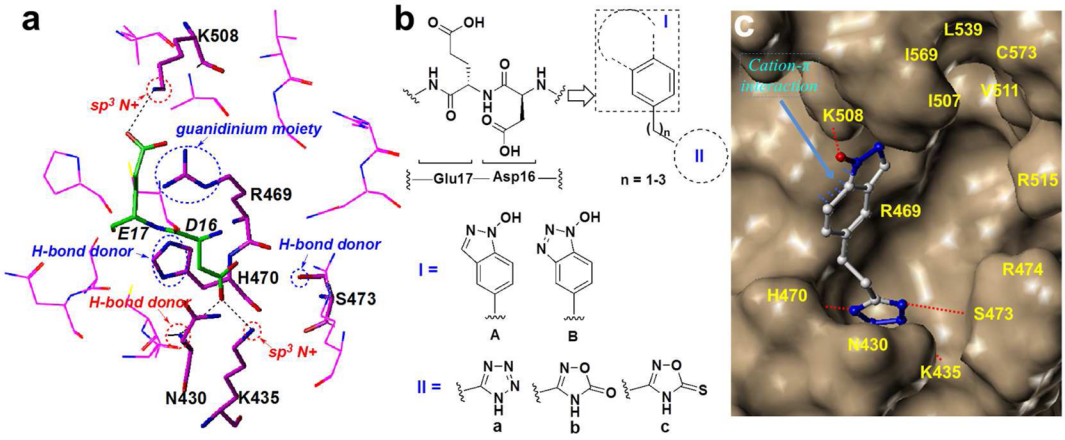

Figure 2. (a) Critical binding elements of β-catenin for inhibitor design. The β-catenin residues are colored magenta. The Tcf4 residues are colored green. D16 and E17 of Tcf4, N430, K435, R469, H470, S473, and K508 of β-catenin are shown as sticks. The critical Tcf-binding elements (red) and the other ligand-binding elements (blue) are shown. (b) Designed molecules to mimic D16 and E17 of human Tcf4. (c) AutoDock predicted binding conformation of **1** (PDB id, 2GL7[12]).

maintain a low level of β-catenin in normal cells. The use of these peptides has a potential to cause cellular toxicities.

Crystallographic and biochemical analyses reveal that three hot spots on β-catenin are critical for binding to Tcf (Figure 1a,b).[9,11,14,20,21] One is K435/K508 where D16/E17 of Tcf4 binds. The second one is K312/K345 where E24/E29 of Tcf4 binds using two alternative conformations.[10,11] The third one is a hydrophobic pocket lined with F253, I256, F293, A295, and I296. V44 and L48 of Tcf4 bind to this pocket. In this study, alanine scanning and surface plasmon resonance (SPR) experiments were conducted to quantify the contribution of each hot spot region. As shown in Figure 1c and Supplementary Figure 1, the K_d value of native β-catenin/Tcf PPIs can be reproduced by the SPR studies. However, no SPR signal was observed for the D16A/E17A mutant (up to 1 μM). The K_d of this mutant is much higher than those of the E24A/E29A and V44A/L48A mutants. The fluorescence polarization (FP) competitive inhibition assay[22] was preformed to further evaluate the importance of these three hot spots (Figure 1d and Supplementary Figure 2). Tcf4 peptide (residues 7−51) has an IC_{50} of 1.09 nM. Under the same assay conditions, the D16A/E17A Tcf4 peptide cannot disrupt β-catenin/Tcf4 PPIs even at a concentration of >200 μM. In contrast, the IC_{50}s of Tcf4 E24A/E29A and V44A/L48A are 68.07 and 606.1 nM, respectively. These studies indicate that D16/E17 of human Tcf4 is much more important than E24/E29 and V44/L48 when binding to β-catenin. We envision that mimicking D16/E17 of human Tcf4 is a valuable starting point to design small-molecule inhibitors for β-catenin/Tcf PPIs.

The key elements of β-catenin for binding to Tcf were then derived, namely, the two sp^3-hybridized nitrogen cations of the side chains of K435 and K508 and the backbone amide nitrogen of N430. These critical binding elements form charge−charge and H-bond interactions with the carboxylic acid groups of Tcf D16 and E17 (Figure 2a). An inspection of the crystal structures of β-catenin in complexes with Tcfs[9−12] identified two additional binding elements that were not used by β-catenin/Tcf PPIs but available for small-molecule binding: (1) the positively charged guanidino moiety of R469; (2) H-bond donors around K435: the imidazole ring of H470 and the hydroxyl group of S473. In the present study, the critical binding elements that anchor side chain carboxylic acids of D16 and E17 of human Tcf4 were initially used for inhibitor design. A bioisostere replacement method described in Supplementary Figures 3−6 was used to design carboxylic acid bioisosteres that better match the critical binding elements. AutoDock 4.2 was performed to prioritize the newly generated fragments.[23] The prioritized fragments were then linked with an assistance of a linker library and Scifinder. As shown in Figure 2b, two carboxylic acid bioisoteres are linked together with the aid of an electron-rich aromatic ring. Indazole-1-ol or benzotriazole-1-ol (pK_a = 4.6−5.6)[24] mimics the carboxyl group of E17 and forms H-bond and charge−charge interactions with β-catenin K508. Under physiological conditions, indazole-1-ol or benzotriazole-

dx.doi.org/10.1021/cb300564v | ACS Chem. Biol. 2013, 8, 524−529

a

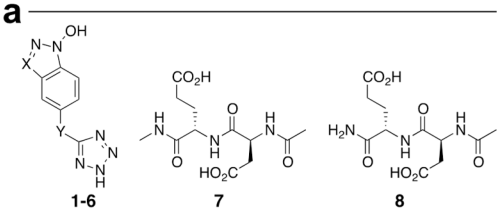

Compounds	X	Y	K_i ± SD (μM)
1	CH	$-CH_2CH_2-$	3.14 ± 0.48
2	N	$-CH_2CH_2-$	54.23 ± 0.36
3	CH	$-CH_2-$	94.17 ± 0.76
4	N	$-CH_2-$	419.01 ± 2.03
5	CH	$-CH_2OCH_2-$	13.55 ± 0.19
6	N	$-CH_2OCH_2-$	155.15 ± 1.17
7			369.59 ± 2.20
8			277.29 ± 3.52
PKF115-584[15]			17.78 ± 2.13
CGP049090[15]			35.56 ± 4.43
PKF118-310[15]			5.82 ± 0.24
PNU74654[16]			180.99 ± 0.68
iCRT3[17]			364.71 ± 6.32
iCRT5[17]			80.34 ± 4.17
iCRT14[17]			53.51 ± 5.24

b

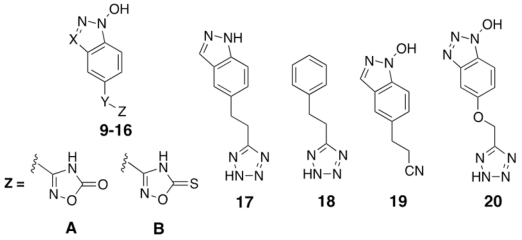

Compounds	X	Y	Z	K_i ± SD (μM)
9	CH	$-CH_2CH_2-$	A	97.74 ± 0.45
10	N	$-CH_2CH_2-$	A	551.25 ± 0.90
11	CH	$-CH_2-$	A	125.16 ± 1.30
12	N	$-CH_2-$	A	165.44 ± 1.45
13	CH	$-CH_2CH_2-$	B	7.24 ± 0.13
14	N	$-CH_2CH_2-$	B	24.36 ± 0.63
15	CH	$-CH_2-$	B	22.46 ± 0.97
16	N	$-CH_2-$	B	105.89 ± 0.18
17				179.93 ± 2.91
18				342.12 ± 6.81
19				115.47 ± 3.09
20				50.40 ± 3.11
Tcf4 (residues 7- 31)				0.074 ± 0.003

Figure 3. (a) FP K_i values of **1**−**8** and seven known inhibitors of β-catenin/Tcf4 PPIs. (b) FP K_i values of **9**−**20** and human Tcf4 (residues 7−31). Each set of data is expressed as mean ± standard deviation (n = 3).

a

β-catenin	K_d (μM)	ΔH (cal/mol)	ΔS (cal/mol•K)	ΔG (kcal/mol)
Wild type	0.531 ± 0.001	-824.023 ± 15.481	25.972 ± 0.067	-8.697 ± 0.026
K435A	4.01 ± 0.08	-317.81 ± 22.11	23.63 ± 0.16	-7.48 ± 0.05
R469A	3.21 ± 0.19	-358.84 ± 9.42	23.94 ± 0.51	-7.62 ± 0.15
K508A	1.59 ± 0.05	-556.83 ± 28.67	24.67 ± 0.26	-8.04 ± 0.07

b

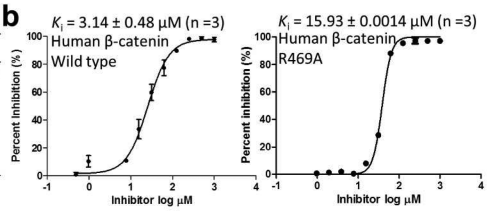

Figure 4. Site-directed mutagenesis to identify key residues that are responsible for the binding affinity of **1** to β-catenin. (a) ITC study of **1** with wild-type and mutant human β-catenin proteins (T = 303.15 K). (b) FP competitive inhibition assay of **1** to disrupt wild-type β-catenin/Tcf4 and β-catenin R469A/Tcf4 interactions.

1-ol is deprotonated and carries a formal charge of −1. The rich p-electrons on the deprotonated indazole-1-ol or benzotriazole-1-ol ring form a favorable cation−π interaction with the positively charged guanidino group of R469. This interaction is not present between Tcf4 and β-catenin. The tetrazole ring (pK_a = 4.5−4.95)[25] was used to replace the carboxyl group of D16 and mimic the charge−charge and H-bond interactions with K435 and N430 of β-catenin. The four lone pairs of the deprotonated tetrazole ring are evenly distributed on the five-membered ring and can form two additional H-bonds with the side chains of H470 and S473. These two H-bonds do not exist in the β-catenin/Tcf complex. Figure 2c and Supplementary Figure 7 show the predicted binding conformation of **1** with β-catenin.

Six compounds, **1**−**6**, were designed and synthesized (Figure 3a and Supplementary Figure 8). The inhibitory activities of these compounds toward disrupting β-catenin/Tcf4 PPIs were determined by the FP assay.[22] Among these six compounds, **1** is the most potent inhibitor with an inhibition constant (K_i) of 3.14 μM (Figure 3a). The K_d of **1** to wild-type β-catenin was determined by isothermal titration calorimetry (ITC). The K_d value and ligand efficiency[26] of **1** are 0.531 μM (Figure 4a) and 0.512, respectively. Compared to a lower K_d value of **1** from the ITC, the higher K_i of **1** to disrupt β-catenin/Tcf4 PPIs in the FP assay was due to a tighter binding between β-catenin and Tcf4. Indazole-1-ol derivatives **1**, **3**, and **5** are more potent than benzotriazole-1-ol derivatives **2**, **4**, and **6** in the FP assay (Figure 3a). It is presumably caused by the electron-withdrawing effect of *N*3 of benzotriazole-1-ol to make this fused ring less electron-rich. The length of linker Y in Figure 3 is also important for inhibitor potency. Two-carbon linker derivatives **1** and **2** are more potent than one-carbon linker derivatives **3** and **4** or CH_2OCH_2 linker derivatives **5** and **6**. In contrast, Tcf4 D^{16}-E^{17} peptides, **7** and **8**, have the K_i values of 396.59 and 277.29 μM, respectively, which are 2 orders of magnitude higher than that of newly designed **1**, indicating that the negatively charged indazole-1-ol and tetrazole moieties not only mimic D16 and E17 of human Tcf4 for the charge−charge and H-bond interactions with β-catenin but also capture additional key binding elements from R469, H470, and S473 of β-catenin. It is worth noting that **1**−**6** were the only compounds initially designed and synthesized. A parallel FP assay demonstrated that **1** was more potent than known inhibitors in Figure 3a.

Site-directed mutagenesis was performed to validate the binding mode of new inhibitors with human β-catenin, as shown in Figure 4. The ITC study shows the K_d of **1** to β-catenin K435A is 4.01 μM, that is 7.6-fold higher than that of **1** with the wild-type β-catenin, and indicates K435 of β-catenin is critical for binding to **1** (Figure 4a and Supplementary Figure 10). The K_d of **1** to β-catenin R469A is 3.21 μM, suggesting that this residue is involved in binding to **1**, although this

dx.doi.org/10.1021/cb300564v | ACS Chem. Biol. 2013, 8, 524−529

mutation does not affect the binding of β-catenin to Tcf4 (Supplementary Figure 9) The ITC study shows the K_d of **1** to human β-catenin K508A is 1.59 μM, indicating this residue is also involved in binding to **1**. Since R469A does not affect β-catenin/Tcf PPIs, the FP assay was performed to validate the binding mode of **1**. The K_i of **1** to the β-catenin R469A mutant/Tcf4 interaction is 15.93 μM (Figure 4b), which is 5-fold less potent than that of **1** to the wild-type β-catenin/Tcf4 PPIs (K_i = 3.14 μM). It again demonstrates the role of R469 in inhibitor binding. The site-directed mutagenesis studies validated the binding mode of **1** with β-catenin shown in Figure 2c.

Further modification was the replacement of the tetrazole ring of **1**−**4** with two other carboxyl bioisosteres, 5-oxo-1,2,4-oxadiazole and 5-thioxo-1,2,4-oxadiazole (pK_a = 6.1−6.7).[27] Compared to tetrazole, 5-oxo-1,2,4-oxadiazole is less acidic and forms weaker charge−charge interactions with β-catenin K435. Correspondingly, **9** and **11** are less potent than **1** and **3**. 5-Thioxo-1,2,4-oxadiazole is more lipophilic and bulkier than 5-oxo-1,2,4-oxadiazole. The better van der Waals contacting with the deep pocket of β-catenin K435 makes **13**−**16** more potent than **9**−**12** and comparable to **1**−**4**. Among **9**−**16**, compound **13** has a K_i of 7.24 μM, providing another good starting point for lead optimization (Figure 3b and Supplementary Figure 8).

Three potent inhibitors identified from the FP assays, **1**, **13**, and **15**, were further tested by the AlphaScreen assay.[22] Concentration-dependent inhibition of **1**, **13**, and **15** was observed (Supplementary Figure 11). Compound **1** displayed a K_i of 7.60 μM and is still the most potent inhibitor among these three. Both the FP and AlphaScreen assays indicate that these inhibitors can completely disrupt β-catenin/Tcf4 PPIs. Since the SPR study shows that the on-rate and off-rate of β-catenin with Tcf are relatively high (3.60×10^6 $M^{-1}s^{-1}$) and slow (0.017 s^{-1}), respectively (Supplementary Figure 1), one question brought to us was whether the new inhibitors can disrupt the preassembled β-catenin/Tcf4 complex or block the binding of monomeric β-catenin to Tcf. To our delight, the K_i values of **1**, **13**, and **15** are independent of the order of addition in the FP assay (Supplementary Figure 12), indicating that the new inhibitors can effectively not only disrupt but also block the tight binding between β-catenin and Tcf4.

Compounds **17**−**20** were designed to further explore the SAR analysis of **1** for disrupting β-catenin/Tcf PPIs and to understand the contribution of each functional group to the binding affinity (Figure 3b and Supplementary Figure 8). The FP competitive inhibition assay shows that the K_i of **17** is 179.93 μM. The pK_a of the indazole NH of **17** is 13.86. This compound cannot be deprotonated under physiological conditions and has no charge−charge interactions with β-catenin K508. Compared to **17**, compound **18** has a poorer inhibitory activity. This is presumably because **17** has more p-electron density on the indazole ring than the phenyl ring of **18**. Therefore, **17** can form a better cation−π interaction with R469. Compared to **1**, compound **19** does not have a tetrazole ring and has a K_i of 115.47 μM, indicating the importance of the tetrazole ring for inhibitor potency. A comparison of the inhibitor activities of **17**, **18**, and **19** also reveals the role of the indazole-1-ol moiety of **1** in inhibitor binding, presumably through forming charge−charge and cation−π interactions with K508 and R469, respectively. Compound **20** is an oxygen-substituted analogue of **2** and has a slightly better inhibitory activity. The electron-donating effect of the phenoxy oxygen in **20** enhances its cation−π interaction with R469. The above SAR analyses are consistent with the proposed binding mode of new inhibitors shown in Figure 2c. The K_i value of human Tcf4 (residues 7−31) is 0.074 ± 0.003 μM.

In summary, this study provides a new bioisostere replacement strategy to rationally design small-molecule PPI inhibitors based on the hot spot residues. The advantage of this approach is that new chemotypes that are drastically different from the structures of the hot spots can be generated for the specific inhibition of PPIs. The discovery of new potent inhibitors that bind to β-catenin and disrupt β-catenin/Tcf PPIs has great therapeutic potential but is very challenging. The critical binding elements around β-catenin K435 and K508 were extracted to design small-molecule inhibitors that bind to coactivator β-catenin and completely disrupt and block β-catenin/Tcf PPIs. A bioisostere design was used to match the critical binding elements and to generate a series of new compounds that mimics D16 and E17 of human Tcf4. The mode of action of new inhibitors with β-catenin was confirmed by the site-directed mutagenesis and SAR studies. Compound **1** has a K_d of 0.531 μM for binding to β-catenin and a K_i of 3.14 μM to completely disrupt β-catenin/Tcf interactions. This compound, with a molecular weight of 230 and a ligand efficiency of 0.512, provides an excellent starting point to generate potent inhibitors specific for the Wnt/β-catenin signaling pathway. Three well-defined pockets are adjacent to K435 and K508 of β-catenin, which can be used for inhibitor optimization. Current research is the evolution of **1** to occupy these three pockets and generate drug-like inhibitors for cell-based and in vivo studies.

METHODS

Fragment Design and Linking. The fragments in Supplementary Figures 3 and 4 were built in the commercially available SYBYL X1.3 software package, and partial atomic charges were calculated using the Gasteiger−Marsili method.[28] The protonation state of β-catenin was set to pH 7.0 when adding the hydrogens. The AMBER 7 force field 99 within SYBYL X1.3 was used to optimize the orientation of hydrogen atoms and the missing side chains of β-catenin and of structural waters. In the AutoDock 4.2 calculations,[23] the grid maps were calculated using AutoGrid with the grid spacing of 0.375 Å. For the fragment docking, any atoms within 6 Å from the proposal critical binding elements (N3+ of K508, the gaunidinium heavy atoms of R469, and N3+ of K435) were used to define the grid box, which leads to two pockets (one includes N3+ of K508 and the gaunidinium group of R469; the second one has N3+ of K435). The binding poses of the fragments that match the proposed binding elements were stored in a SYBYL molecular database. The distance between each fragment of two pockets was measured, and the linkers in Supplementary Figure 6 were merged to generate the ligand structure. For the ligand docking study, the dimensions of the grid box were 39 × 28.5 × 21.5 Å to include three critical binding elements. Docking was performed using the Lamarckian genetic algorithm (LGA), and the pseudo-Solis and Wets method was applied for the local search. Each docking experiment was performed 100 times, yielding 100 docked conformations. Other settings were the standard default parameters. The results of the docking experiments were evaluated by the auxiliary clustering analysis and a visual inspection to match the proposed critical binding elements.

Fluorescence Polarization Assays. Experiments were performed in 96-well Microfluor 2 black plates on a Synergy 2 plate reader (Biotek). The polarization was measured at RT with an excitation wavelength at 485 nm and an emission wavelength at 535 nm. The FP experiments were performed in an assay buffer of 137 mM NaCl, 2.7 mM KCl, 10 mM Na_2HPO_4, 2 mM KH_2PO_4, 100 μg/mL of bovine gamma globulin, and 0.01% Triton-X 100. The final reaction volume was 100 μL. In the FP saturation experiments, different concentrations

dx.doi.org/10.1021/cb300564v | ACS Chem. Biol. 2013, 8, 524−529

of wild-type or mutant β-catenin (residues 142−686) was incubated with 2.5 nM C-terminally fluorescein-labeled human Tcf4 (residues 7−51). The apparent K_d values of β-catenin with Tcf4 were determined. In the FP competitive inhibition assays, 10 nM β-catenin was incubated with 2.5 nM Tcf4 fluorescence tracer for 30 min at 4 °C, and then, different concentrations of the tested peptides or compounds were added. For each inhibitor competition assay, the negative control (equivalent to 0% inhibition) refers to 2.5 nM Tcf4 fluorescence tracer and 10 nM β-catenin in the assay buffer without tested compound presenting. The positive control (equivalent to 100% inhibition) refers to only 2.5 nM Tcf4 fluorescence tracer in the assay buffer. Each assay plate was covered black and gently mixed on an orbital shaker for 3 h before testing. The background of the tested peptides or inhibitors was corrected by subtracting the raw intensity values of the sample background well (all components except probe) from the raw intensity values of the corresponding test wells (all components). The IC_{50} values were determined by nonlinear least-squares analysis using GraphPad Prism 5.0. The K_i values were derived from the IC_{50} values by the reported method.[29] Experiments were carried out in the presence of 1% DMSO.

■ ASSOCIATED CONTENT

Supporting Information

Supplementary Figures 1−12, Supplemantary Schemes 1−3, Supplementary Methods, and the NMR spectra of compounds **1**−**20**. This material is available free of charge *via* the Internet at http://pubs.acs.org.

■ AUTHOR INFORMATION

Corresponding Author

*Phone: 801-581-6747. E-mail: markji@chem.utah.edu.

Notes

The authors declare no competing financial interest.

■ ACKNOWLEDGMENTS

This work was in part supported by the Pulmonary Fibrosis Foundation I. M. Rosenzweig Young Investigator Award (Award number, 235170). We would like to thank D. P. Goldenberg at the University of Utah for use of his isothermal titration calorimetry instrument, W. Xu at the University of Washington for β-catenin cDNA, H. Liu at St. Andrew University, U.K., for the pEHISTEV vector, and the Center for High Performance Computing at the University of Utah for computer time.

■ REFERENCES

(1) Wells, J. A., and McClendon, C. L. (2007) Reaching for high-hanging fruit in drug discovery at protein−protein interfaces. *Nature 450*, 1001−1009.

(2) Clackson, T., and Wells, J. A. (1995) A hot spot of binding energy in a hormone−receptor interface. *Science 267*, 383−386.

(3) Mysinger, M. M., Weiss, D. R., Ziarek, J. J., Gravel, S., Doak, A. K., Karpiak, J., Heveker, N., Shoichet, B. K., and Volkman, B. F. (2012) Structure-based ligand discovery for the protein-protein interface of chemokine receptor CXCR4. *Proc. Natl. Acad. Sci. U.S.A. 109*, 5517−5522.

(4) He, M. M., Smith, A. S., Oslob, J. D., Flanagan, W. M., Braisted, A. C., Whitty, A., Cancilla, M. T., Wang, J., Lugovskoy, A. A., Yoburn, J. C., Fung, A. D., Farrington, G., Eldredge, J. K., Day, E. S., Cruz, L. A., Cachero, T. G., Miller, S. K., Friedman, J. E., Choong, I. C., and Cunningham, B. C. (2005) Small-molecule inhibition of TNF-α. *Science 310*, 1022−1025.

(5) Ding, K., Lu, Y., Nikolovska-Coleska, Z., Qiu, S., Ding, Y., Gao, W., Stuckey, J., Krajewski, K., Roller, P. P., Tomita, Y., Parrish, D. A., Deschamps, J. R., and Wang, S. (2005) Structure-based design of potent non-peptide MDM2 inhibitors. *J. Am. Chem. Soc. 127*, 10130−10131.

(6) Czarna, A., Beck, B., Srivastava, S., Popowicz, G. M., Wolf, S., Huang, Y., Bista, M., Holak, T. A., and Dömling, A. (2010) Robust generation of lead compounds for protein−protein interactions by computational and MCR chemistry: p53/Hdm2 antagonists. *Angew. Chem., Int. Ed. 49*, 5352−5356.

(7) Buckley, D. L., Van Molle, I., Gareiss, P. C., Tae, H. S., Michel, J., Noblin, D. J., Jorgensen, W. L., Ciulli, A., and Crews, C. M. (2012) Targeting the von Hippel-Lindau E3 ubiquitin ligase using small molecules to disrupt the VHL/HIF-1α interaction. *J. Am. Chem. Soc. 134*, 4465−4468.

(8) Clevers, H., and Nusse, R. (2012) Wnt/β-catenin signaling and disease. *Cell 149*, 1192−205.

(9) Graham, T. A., Weaver, C., Mao, F., Kimelman, D., and Xu, W. (2000) Crystal structure of a β-catenin/Tcf complex. *Cell 103*, 885−896.

(10) Poy, F., Lepourcelet, M., Shivdasani, R. A., and Eck, M. J. (2001) Structure of a human Tcf4-β-catenin complex. *Nat. Struct. Biol. 8*, 1053−1057.

(11) Graham, T. A., Ferkey, D. M., Mao, F., Kimelman, D., and Xu, W. (2001) Tcf4 can specifically recognize β-catenin using alternative conformations. *Nat. Struct. Biol. 8*, 1048−1052.

(12) Sampietro, J., Dahlberg, C. L., Cho, U. S., Hinds, T. R., Kimelman, D., and Xu, W. (2006) Crystal structure of a β-catenin/BCL9/Tcf4 complex. *Mol. Cell 24*, 293−300.

(13) Sun, J., and Weis, W. I. (2011) Biochemical and structural characterization of β-catenin interactions with nonphosphorylated and CK2-phosphorylated Lef-1. *J. Mol. Biol. 405*, 519−530.

(14) Knapp, S., Zamai, M., Volpi, D., Nardese, V., Avanzi, N., Breton, J., Plyte, S., Flocco, M., Marconi, M., Isacchi, A., and Caiolfa, V. R. (2001) Thermodynamics of the high-affinity interaction of TCF4 with β-catenin. *J. Mol. Biol. 306*, 1179−1189.

(15) Lepourcelet, M., Chen, Y.-N. P., France, D. S., Wang, H., Crews, P., Petersen, F., Bruseo, C., Wood, A. W., and Shivdasani, R. A. (2004) Small-molecule antagonists of the oncogenic Tcf/β-catenin protein complex. *Cancer Cell 5*, 91−102.

(16) Trosset, J.-Y., Dalvit, C., Knapp, S., Fasolini, M., Veronesi, M., Mantegani, S., Gianellini, L. M., Catana, C., Sundström, M., Stouten, P. F. W., and Moll, J. K. (2006) Inhibition of protein-protein interactions: the discovery of druglike β-catenin inhibitors by combining virtual and biophysical screening. *Proteins 64*, 60−67.

(17) Gonsalves, F. C., Klein, K., Carson, B. B., Katz, S., Ekas, L. A., Evans, S., Nagourney, R., Cardozo, T., Brown, A. M., and DasGupta, R. (2011) An RNAi-based chemical genetic screen identifies three small-molecule inhibitors of the Wnt/wingless signaling pathway. *Proc. Natl. Acad. Sci. U.S.A. 108*, 5954−5963.

(18) Tian, W., Han, X., Yan, M., Xu, Y., Duggineni, S., Lin, N., Luo, G., Li, Y. M., Han, X., Huang, Z., and An, J. (2012) Structure-based discovery of a novel inhibitor targeting the β-catenin/Tcf4 interaction. *Biochemistry 51*, 724−731.

(19) Grossmann, T. N., Yeh, J.-H. T., Bowman, B. R., Chu, Q., Moellering, R. E, and Verdine, G. L. (2012) Inhibition of oncogenic Wnt signaling through direct targeting of β-catenin. *Proc. Natl. Acad. Sci. U.S.A. 109*, 17942−17947.

(20) von Kries, J. P., Winbeck, G., Asbrand, C., Schwarz-Romond, T., Sochnikova, N., Dell'Oro, A., Behrens, J., and Birchmeier, W. (2000) Hot spots in β-catenin for interactions with LEF-1, conductin and APC. *Nat. Struct. Biol. 7*, 800−807.

(21) Gail, R., Frank, R., and Wittinghofer, A. (2005) Systematic peptide array-based delineation of the differential β-catenin interaction with Tcf4, E-cadherin, and adenomatous polyposis coli. *J. Biol. Chem. 280*, 7107−7117.

(22) Zhang, M., Huang, Z., Yu, B., and Ji, H. (2012) New homogeneous high-throughput assays for inhibitors of β-catenin/Tcf protein−protein interactions. *Anal. Biochem. 424*, 57−63.

(23) Morris, G. M., Huey, R., Lindstrom, W., Sanner, M. F., Belew, R. K., Goodsell, D. S., and Olson, A. J. (2009) AutoDock4 and

AutoDockTools4: Automated docking with selective receptor flexibility. *J. Comput. Chem. 30*, 2785−2791.
(24) Subirós-Funosas, R., Prohens, R., Barbas, R., El-Faham, A., and Albericio, F. (2009) Oxyma: an efficient additive for peptide synthesis to replace the benzotriazole-based HOBt and HOAt with a lower risk of explosion. *Chem.—Eur. J. 15*, 9394−9403.
(25) Herr, R. J. (2002) 5-Substituted-1*H*-tetrazoles as carboxylic acid isosteres: medicinal chemistry and synthetic methods. *Bioorg. Med. Chem. 10*, 3379−3393.
(26) Hopkins, A. L., Groom, C. R., and Alex, A. (2004) Ligand efficiency: a useful metric for lead selection. *Drug Discovery Today 9*, 430−431.
(27) Kohara, Y., Kubo, K., Imamiya, E., Wada, T., Inada, Y., and Naka, T. (1996) Synthesis and angiotensin II receptor antagonistic activities of benzimidazole derivatives bearing acidic heterocycles as novel tetrazole bioisosteres. *J. Med. Chem. 39*, 5228−5235.
(28) Gasteiger, J., and Marsili, M. (1980) Iterative partial equalization of orbital electronegativity: a rapid access to atomic charges. *Tetrahedron 36*, 3219−3228.
(29) Nikolovska-Coleska, Z., Wang, R., Fang, X., Pan, H., Tomita, Y., Li, P., Roller, P. P., Krajewski, K., Saito, N. G., Stuckey, J. A., and Wang, S. (2004) Development and optimization of a binding assay for the XIAP BIR3 domain using fluorescence polarization. *Anal. Biochem. 332*, 261−273.